2008

Optimization of Membrane Networks: Superstructures

By Nina Wright and Ernest West

Univ. of Oklahoma

5/2/2008

Abstract

The current rising cost of energy is driving technology towards more economical means of providing fuel that is more affordable and hopefully more environmentally friendly. One example of this phenomenon is the new technology that is under consideration for widespread implementation in natural gas processing. Current research is being proposed to improve membrane technology as such to allow for a more industrial sized usage of membranes or membrane networks, since most usage of membranes today is limited to smaller scale separation processes.

However, the cellulose acetate membrane has proven capable of handling industrial sized amounts of gas separation, if the membrane is kept from plasticization. Minimizing the cost of membrane networks is another way to save on economic costs, and this is accomplished through the design and modeling of membrane superstructures.

Membrane superstructure models allow one to enter various parameters and variables into a model and then the result will be the most favorable and efficient design of membrane networks. The superstructure model that was solved in this paper involved solving a model for the separation of carbon dioxide from methane, while specifying the permeability of both components and the tube side and shell side pressure of each component. The ultimate objective was to minimize the cost of the structure by minimizing various components of the superstructure, namely the area, power of the compressors, and the amount of CO_2 that remains in the retentate of the membranes. The superstructure membrane model was evaluated by using a mixed integer non-linear programming model which was designed to find the most cost-effective arrangement of a membrane separation network. The results showed an optimum two membrane network with partial recycle of the retentate from the first membrane to the second membrane and partial recycle of the permeate of the second membrane to the feed of the first. The cost of the resulting model was \$11.05 for every $1000m^3$ of feed processed.

Table of Contents

Introduction

The natural gas industry is one of the largest industries in the United States with 10,000 companies producing an annual revenue of $100 billion dollars per year. Actual natural gas processing is the largest application of industrial gas separation. While membrane processes have less than 1% of this market. (Baker, 2002)

Membranes have been introduced as an alternative to traditional natural gas processing. In the interest of conserving energy costs and environmental concerns membranes offer a new exciting alternative to traditional natural gas processing. Energy consumption in the United States is consistently increasing with a total natural gas energy consumption of 21.34 tcf/year. (US Energy,1998)

Reductions in energy consumption are of strategic importance, because they reduce U.S. dependence on foreign energy supplies. Improving the energy efficiency of production technology can lead to increased productivity and enhanced competitiveness of U.S. products in world markets. Processes that use energy inefficiently are also significant sources of environmental pollution.

In 1987, the total energy consumption of all sectors of the U.S. economy was 76.8 quads, of which approximately 29.5 quads, or 38% was used by the industrial sector, at a cost of $100 billion. A cheaper method of producing pipeline quality natural gas is through the use of membranes.

An example of membranes already used in industry is the natural gas processing plant in Qadirpur, Pakistan. The membrane plant was installed by UOP in 1995 and in 1999 it was the largest membrane based gas plant in the world. It is designed for 265 MMSCFD gas flow at 59 bar. The CO_2 content in the natural gas is reduced from 6.5 % to less than

2% and provides gas dehydration to pipeline specifications. The membrane used is a cellulose acetate membrane. (Dortmundt, UOP, 1999)

Also, exciting new strides are being made in membrane technology. At the University of Texas in Austin, new "thermally rearranged" plastic membranes have been developed which have 4 times higher selectivity and 100 times more throughput than the currently standard cellulose acetate membranes. In addition, they have greatly improved thermal stability, being usable at temperatures over 600°F, a barrier formerly not crossed in membrane separation technology. Using such a membrane would reduce the amount of space needed for the CO_2 removal unit in natural gas processing plants by a factor of 500. Such advances show great promise in being more efficient in cost, space, and recovery than conventional processes and foreshadow much more prevalent use of membranes.

1. Background

A membrane is a physical barrier from semi-permeable material that allows some component to pass through while others are held back. A feed consisting of a mixture of two or more components is separated in which one or more species move faster than the other. The part of the feed that move through the membrane is called the permeate as shown in **Figure 1**. The part of the feed that does not pass through is called the retentate. One of the earliest gas-separation membrane used commercially was from Monsanto in 1979 with the introduction of a hollow-fiber membrane made of polysulfone to separate certain gas mixtures (Seader, 1990). Some other industrial applications of membranes have included reverse osmosis, dialysis, microfiltration, and ultrafiltration.

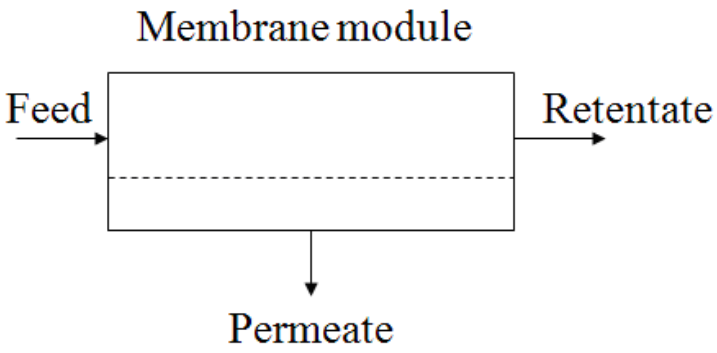

Figure 1: Membrane Model

1.2 Membrane Material

The first membranes used commercially were uniform in structure and had very low flow rates (Howell, 1990). In principle all types of materials can be used as membranes. However, the selection of a type of material is dependent on the cost, on the separation task, the desired structure of the membrane and the operating conditions under which it has to perform. Membrane materials are normally divided into biological, and synthetic. The most commonly used membrane materials are organic polymers. There are a large number of polymer materials available. Cellulose acetate is widely used in natural gas processing because of it high selectivity of carbon dioxide over methane (Seader, 1998). Some of the advantages of polymers are flexibility, permeability and ability to be formed into a variety structures. However, polymers are generally not thermally stable, which can be a problem for many separation tasks. Inorganic membrane materials are starting to become more important. They are much more chemically and thermally stable then

polymers, but have been limited in their use, mainly due to the expense of the material. Inorganic membranes are commonly used in gas-separation.

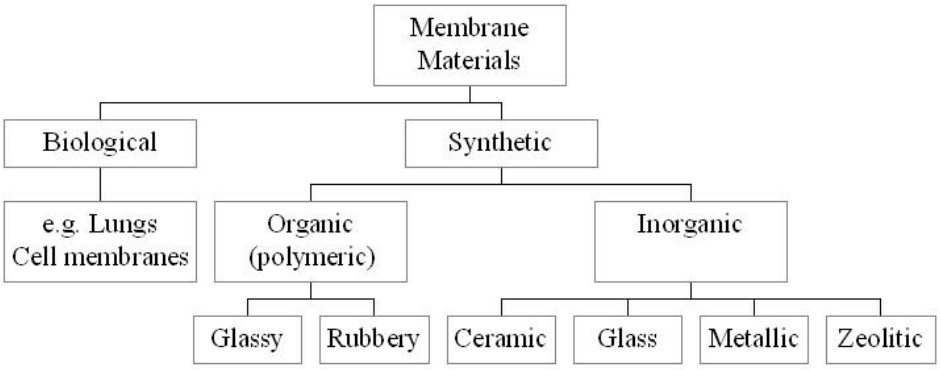

Figure 2: Membrane Materials

1.3 Membrane Structure

There are three main types of membranes structures: porous, non-porous, and carrier. In porous membranes the selectivity is mainly decided due to the size of the pores. These types of membranes are used in microfiltration and in ultrafiltration. The non-porous membranes are normally used in gas separation and pervaporation. In these membranes the molecules first dissolves into the membrane and then diffuse through it. The separation is based on how well different compounds dissolve and diffuse through the membrane. Some molecules diffuse fast and others diffuse slowly as shown in **Figure 3**. In the carrier transport membranes a specific carrier molecule facilitates the transport of a specific molecule though the membrane. This kind of transport occurs for example in the lipid bilayer of a cell. The carrier mediated transport is very selective and can be used to remove components like gases, liquids and ionic or non-ionic components.

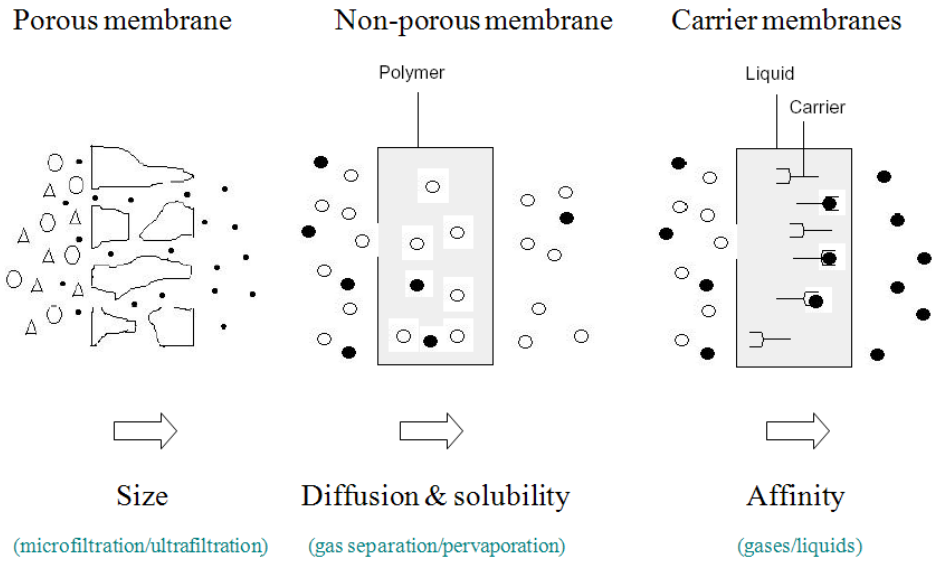

Figure 3: Membrane Porosity (Mulder, 1996)

Membrane materials are usually made as thin as possible to increase the permeability, which is the ability of a chemical to pass through a material. However, this makes the membrane very fragile. In order to overcome this problem the membranes are made with an asymmetric structure where the thin selective nonporous layer is grafted on a thicker porous layer of the same material as shown in **Figure 4**. This porous layer provides the stability and allows a free flow of the compounds that permeate through the selective layer.

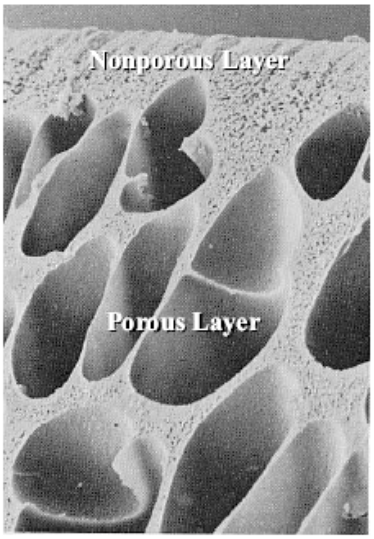

Figure 4: Porous and Nonporous Layers (Dortmundt, 1999)

1.4 Membrane Theory

Membrane processes can be thought of as a simple separation technique which employ the membrane as a partitioning phase. In the process, a driving force, usually pressure or concentration, is applied to one side of the membrane and the selective components pass to the other side as the permeate. Mass transport through membranes can be described by Fick's Law as shown in the following:

$$N_i = \frac{q_i}{A} = \frac{D_i(c_{io} - c_{iL})}{l} \qquad \textbf{Eq. 1}$$

Where

N_i = molar flux of the component i

q_i = molar flow rate of component i

A = active area of the membrane

D_i = diffusivity of component i

c_{io} = concentration of component i on the feed side

c_{iL} = concentration of component i on the permeate side

l = the membrane thickness

However, Fick's Law is not universal. In each phase it is true, but near the interface it is not true. Diffusivity is a measure of the mobility of the molecules in the membrane. If the thermodynamic equilibrium is assumed to exist at the two membrane interfaces, the concentrations in Fick's law can be related to the partial pressures by Henry's Law, which is a linear relations written as:

$$c_i = H_i * p_i \qquad \textbf{Eq. 2}$$

Where

c_i = is the concentration of component i

H_i = solubility constant

p_i = partial pressure of component i

Solubility indicated how much gas can be taken up by the membrane. Using Henry's Law for equilibrium of molecules, Fick's law can then be modified to another form that relates the flux with pressure instead of concentration. The solubility constant is assumed

to be independent of the total pressure and the temperature is assumed to be the same at both side of the membrane.

$$\frac{q_i}{A} = \frac{P_{Mi}(p_{io} - p_{iL})}{l} \qquad \textbf{Eq. 3}$$

$$P_{Mi} = H_i * D_i \qquad \textbf{Eq. 4}$$

Where P_{Mi} is called the permeability of the membrane and it depends on both the solubility and the diffusivity of component i. This equation shows that in order to achieve a high flux, a thin membrane should be used and the feed side pressure should be set at a high level.

The separation factor measures the membrane's ability to separate two components in a binary system. The separation factor is also called selectivit and is usually written in the following form:

$$\alpha_{A,B} = \frac{y_A / x_A}{y_B / x_B} \qquad \textbf{Eq.5}$$

Where

$\alpha_{A,B}$ = separation factor

A = component A

B= component B

y_i = the mole fraction in the permeate leaving the membrane

x_i = the mole fraction in the retentate

on the feed side of the membrane

Typical membrane materials show an inverse relationship between permeability and selectivity. An ideal membrane would incorporate high permeability with high selectivity. This can be accomplished by using with a highly selective membrane and make it as thin as possible to increase the permeability.

1.5 Membrane Modules

Membranes are produced in a large variety of shaped which is formed into modules. They are designed in a way as to minimize the total volume while allowing the fluids to sufficiently flow through to prevent excessive deposits on the membrane. Membranes modules are divided into two main categories: flat sheets and tubular. As show in **Figure 5**, flat sheets can be molded into either a plate or spiral shape. Tubular membranes are categorized on the diameter lengths of each tube. The two most common modules used in the natural gas industry are spiral-wound and hollow fiber (Howell, 1990).

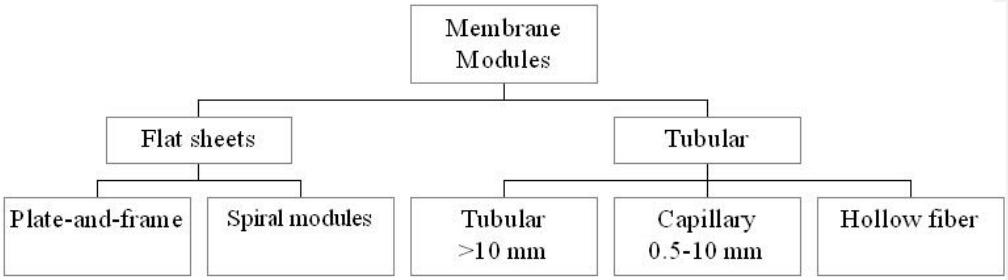

Figure 5: Membrane Modules

1.6 Spiral-wound Modules

A spiral-wound module is made from a membrane laid out flat with spacers, passages, and barriers on both sides to distribute the feed and to collect the permeate. The sheet is wound into a spiral and placed in a metal enclosure. The basic concept is to pack a large area into a small volume. These membranes are usually operated in the cross-flow mode. **Figure 6** shows a representation of a spiral-wound membrane.

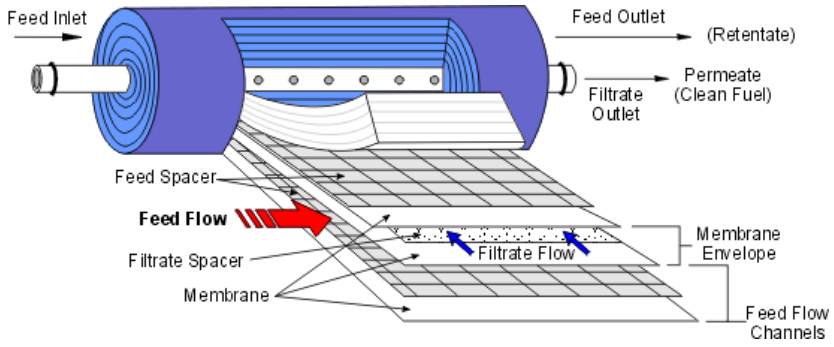

Figure 6: Spiral-Wound Module (Filtrations Solutions Inc.)

A disadvantage to spiral-wound is that is has the lowest cost per area ratio when compared to other membranes. They are difficult to clean because they cannot be unwrapped without the glue line seal being ruptured. They are more prone to fouling than tubular and some plate and frame units, however they are more resistant to fouling than hollow fibers (Porter, 1990).

1.7 Hollow Fiber Module

Hollow fiber belong to the tubular membrane modules with having a diameter less than 0.5 millimeters. Most gas-separation membranes are formed into hollow-fiber modules due to their low production cost (Kookos, 2002). Hollow fiber is favored in gas-separation because of its high separation areas and selectivity. The hollow fiber configuration has an advantage over spiral-wound in that it offers the highest membrane surface area per unit volume ratio. It can packed up to five times as much membrane area into the same volume. The best selectivity is achieved with the membrane operating in a couter-current regime (Howell, 1990). A major disadvantage is that hollow fiber configuration is more susceptible to fouling and plugging than any of the other three configuration. (Porter, 1990). **Figure 7** show a cross section of a single tube. **Figure 7** show a hollow fiber membrane made by Aquilo Gas Separation. While **Figure 8** shows a hollow fiber membrane bundle, as seen in industrial sized gas-gas separators.

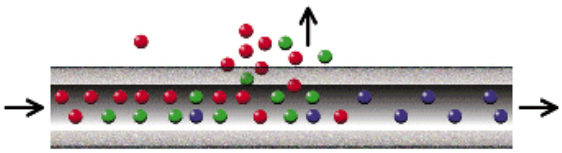

Figure 7:Hollow Fiber Membrane Module (Aquilo Gas Separation)

Figure 8: Hollow Fiber Membrane Bundle (Aquilo Gas Separation)

2. Natural Gas Processing

Natural gas treatment is the largest application of industrial gas separations. Membrane processes should have large potentials as they so far have less than 1 % of this market. (Baker,2002). **Figure 9** shows a process diagram of a typical natural gas plant. The natural gas comes up from the well and goes through a number of processing steps: wellhead dehydration, acid (sour) gas removal in dehydration and in treatment of the hydrocarbon products. It may even be used for the separation of the hydrocarbons.

Natural gas composition varies from place to place. Methane is the major component. Typically, it is 75-90 % of the total composition. Natural gas also contains significant amounts of ethane, some propane and butane, and 1-3 % other higher hydrocarbons. The

undesirable products are water, carbon dioxide, and nitrogen and hydrogen sulfide. (Natural Gas Supply Association, 2008)

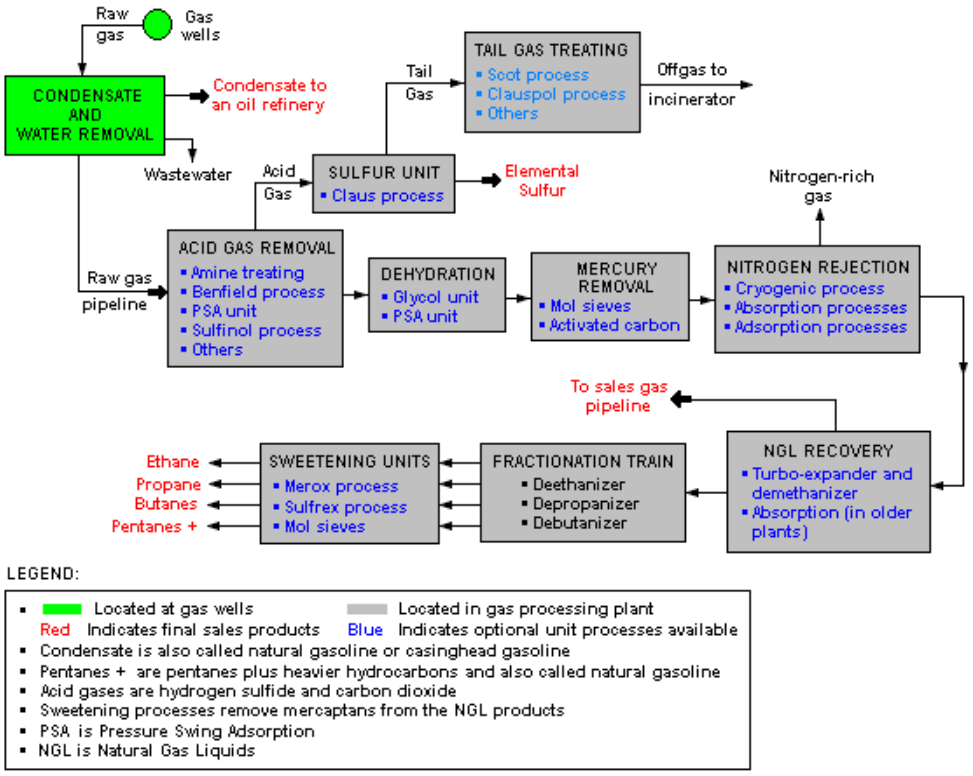

Figure 9: Process Diagram of a Natural Gas Process (Wikipedia, 2008)

The removal of CO_2 from gas streams is typically found in the purification of natural gases, the separation of CO_2 in enhanced oil recovery processes, removal of CO_2 from flue gas and the removal of CO_2 from biogas. The purification of natural gas is often referred to as gas sweetening. Natural gas contains a number of undesirable impurities.

As a part of gas treatment the gas is dehydrated and the sour gases, the CO_2 and hydrogen sulfide, are removed. The reason is to increase the heating value of the natural gas. Pipeline requires natural gas to contain less than 2% CO_2. The pipeline specifications are tight and most natural gas requires some treatment. The other reasons for gas sweetening are to reduce corrosion and prevent pollution of sulphur dioxide which is generated during the combustion of natural gas containing hydrogen sulfide.

The most common process for removal of CO_2 from natural gas is absorption using amines. Currently Amine treating is used in 95% of U.S. gas sweetening operations (Natural Gas Supply Association, 2008). This involves an absorption column where CO_2 is removed from the natural gas and a stripping column where the amine solution is regenerated. Other methods available are cryogenic distillation, membranes and hybrid processes where membranes are integrated with the absorption system.

2.1 Market in Natural Gas Industry

Currently there are a few materials that are used for more than 90 % of all membrane gas separations. The most common membrane modules are hollow-fibre modules and a very common polymer is cellulose acetate. (Baker, 2002)

There are three "markets" for the natural gas treatment. In low gas volume (< 5 MSCF/d), membranes are very attractive. In moderate systems (5-40 MSCF/d), the attractiveness of the amine and membrane systems compete. In high volume systems (>40 MSCF/d), membrane systems are too expensive to compete with amine systems.

Also in high volume, there is a problem with low selectivity and flux. There are also some hybrid solutions where membranes are used together with conventional amine systems. (Baker, 2002)

2.2 Membrane Advantages

Membranes are simpler, smaller and lighter systems compare with the existing separation solutions for CO_2 removal. This is especially important for offshore applications. They are cleaner, use less chemical additives and have lower energy consumption than the conventional absorption process. They are therefore a better environmental solution. C O2 and hydrogen sulfide are the faster diffusing gases and using membranes they are removed at the same time. It is also possible to remove water vapor in the same step. Other factors are safety advantages, less maintenance, lower capital and operating costs (for small to medium systems) and a possibility to treat the gas at the wellhead.

2.3 Membrane Disadvantages

The main disadvantage of membrane systems is that low selectivity and flux means that they are not economically viable for large scale gas separations. The thermal stability of the existing polymer membranes can also be a problem. Also degradation of the membrane can lead to a short lifespan.

3. Development of Model

The model for the single membrane was the initial step in formulating the model of the superstructure. The model was based off of the paper written by Ionannis K. Kookos,

entitled: A targeting approach to the synthesis of membrane networks for gas separation. The paper models a membrane shown in **Figure 10**. In this figure the membrane is divided into multiple sections and the retentate and permeate are flowing counter current to one another. The main equations used to model this two component, counter current flow through the membrane include performing a component material balance, rate of transport equation, and the mole fractions of each component.

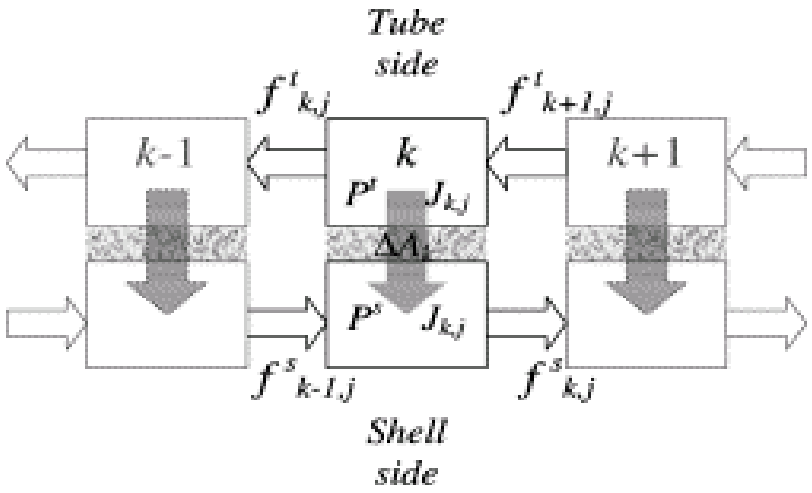

Figure 10: Simplified Representation of Membrane Model (Kookos, 2002)

Table 1: Equations for Single Membrane Counter Current Flow

Tube side Component Material Balance:	$f^{t}_{k,j} = f^{t}_{k+1,j} - J_{k,j}\Delta A_k$
Shell side Component Material Balance	$f^{s}_{k,j} = f^{s}_{k-1,j} + J_{k,j}\Delta A_k$
Active Area of Membrane Segment	$\Delta A_k = N_t \pi d_{lm} d_{zk}$
Log Mean Diameter	$d_{lm} = \frac{(d_o - d_i)}{\ln(d_o/d_i)}$
Flux through Membrane	$J_{k,j} = \frac{Q_j}{\delta_m}\left(x^{t}_{k,j} P^t - x^{s}_{k,j} P^s\right)$
Tube side Mole fraction of Component	$x^{t}_{k,j} = \frac{f^{t}_{k,j}}{\Sigma^{NC}_{l=1} f^{t}_{k,l}}$
Shell side Mole fraction of Component	$x^{s}_{k,j} = \frac{f^{s}_{k,j}}{\Sigma^{NC}_{l=1} f^{s}_{k,l}}$

Component Material Balances are described by $f^{t}_{k,j}$, and $f^{s}_{k,j}$. These molar flow rates represent the component material balances of the tube and shell side with respect to (k=1,2,….,NP) the number of sections and (j=1,2,…,NC) the number of components.

While ΔA_k is the active area of the membrane segment (k). In order to calculate the area the log mean diameter is needed and is represented by d_{lm}. The segment length must also be specified, and is represented by d_{zk}. While (z) is the segment length of segment (k).

The flux through the membrane segment is represented by $J_{k,j}$, and to determine this value the permeability of each component Q_j is defined as well as the thickness of the membrane δ_m. The mole fractions of each component on the tube and shell side are represented by $x^t_{k,j}$, and $x^s_{k,j}$.

When these equations are put into GAMS it is a nonlinear model as the equations to determine the variables are multiplied by other variables. One way to solve this problem is to discretize the variables of the component material balance, shell side and tube side, and the tube and shell side mole fractions of each component. Discretization was accomplished by allowing the variable to be divided into many different parts; an example of the discretized mole fraction of component j is as follows:

```
lowerboundMFJTube(k,j,d,m) ..ft(k,j,m)=G=(sigT(k,m))*dxt(d)-100*(1-yt(k,j,d,m)) ;
upperboundMFJTube(k,j,d,m) ..ft(k,j,m)=L=(sigT(k,m))*dxt(d+1)+feed(j)*(1-yt(k,j,d,m)) ;
discreteMFJTube(k,j,m)     ..sum(d,yt(k,j,d,m))=E=sum(ka$(ord(ka)>ord(k)),yk(ka,m));
```

The discretization variable (yt) is the number of segments that compose the divided variable. The discretization of the variable allows GAMS to search for a solution that is feasible along linear terms, instead of non linear.

Once the model was deemed feasible the data from the model was exported to excel in order to visualize the inner workings of the membrane, and to see if the results matched what was expected.

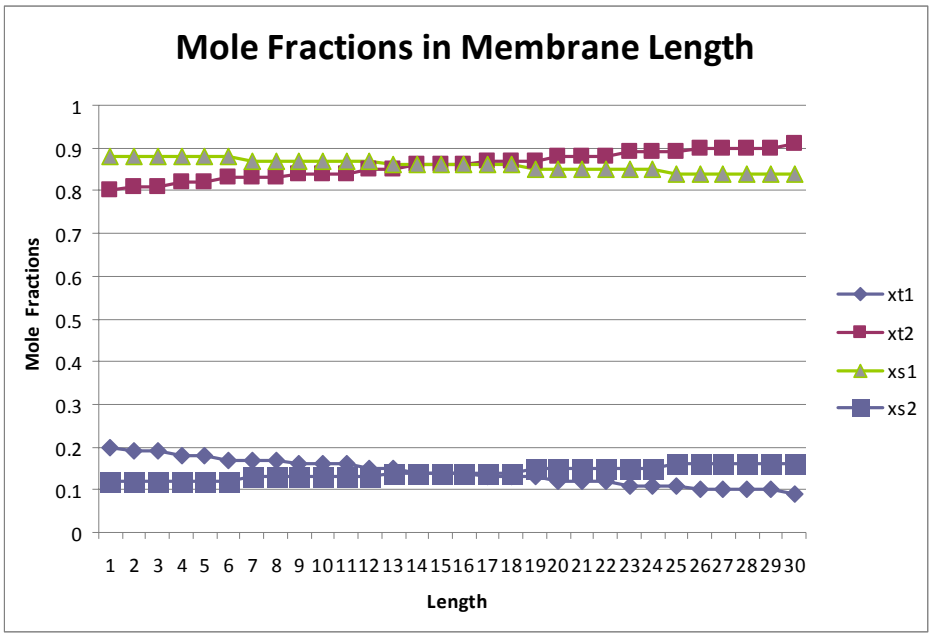

Graph 1: Mole Fractions vs. Length

In Graph 1 the mole fractions of carbon dioxide (1), and methane (2) are shown along the length of the membrane. Ideally, the mole fraction of CO_2 on the tube side should decrease as length increases and the mole fraction of methane on the tube side should increase with increasing length. The opposite trend should happen for the shell side. This trend is confirmed with the Graph 1, and therefore the model in GAMS can be confirmed as reliable.

Other graphs were also able to confirm the reliability of the GAMS model from the extruded data, the partial pressure of Carbon dioxide and methane were able to be determined. The partial pressure drop of both of these components were required to go from a larger value to a smaller value according Fick's Law and the proper driving force. Without this confirmation the model would be considered obsolete.

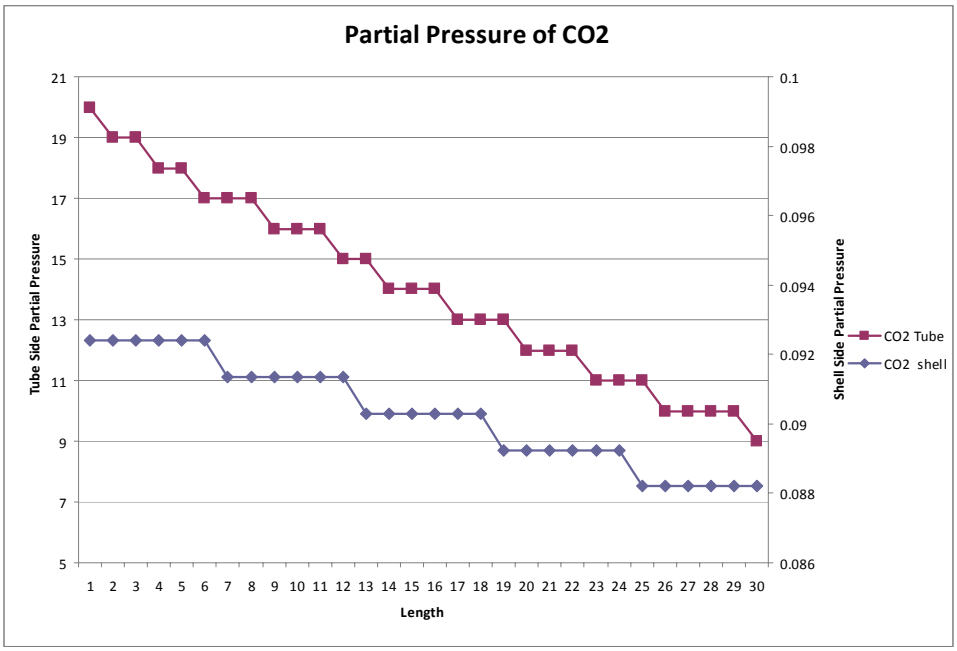

Graph 2: Partial Pressure of CO_2 in membrane

Graph 2 shows the driving force through the hollow fiber membrane with the tube side partial pressure exceeding the shell side. This trend is followed by the methane as well as can be seen from Graph 3. The apparent flat sloped sections of the graph can be explained by the discretization of the variables, the linearized variables do not reflect any change in pressure drop, as the variable is constant for a small portion of the modeling process.

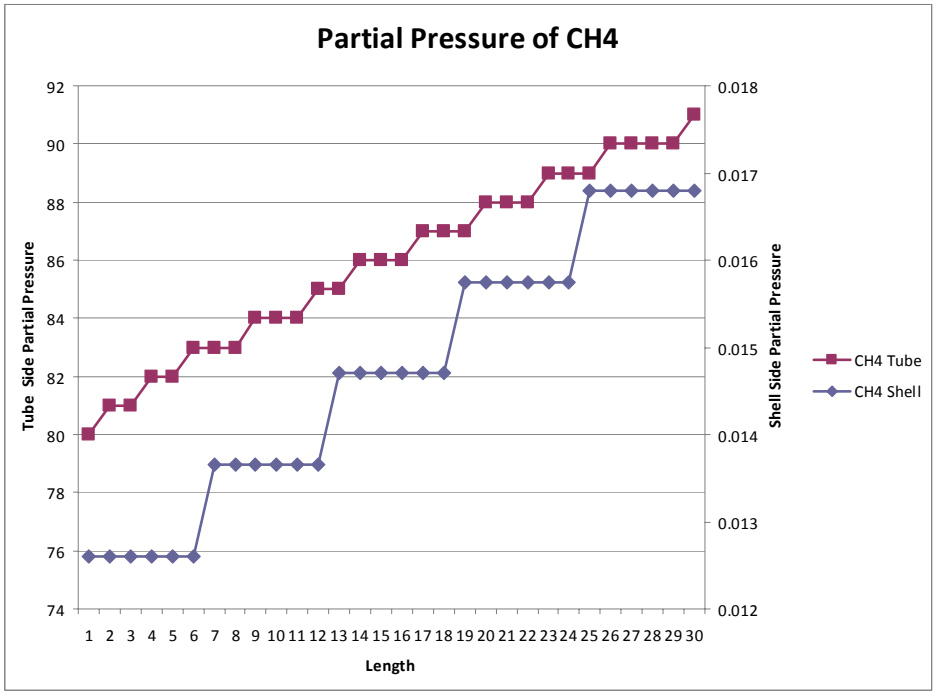

Graph 3: Partial Pressure of Methane in Membrane

4. Superstructure

A superstructure approach to process design is used in this project as a mathematical optimization problem for a network of membranes. A superstructure is a representation that contains all possible design configurations that are considered candidates for the optimal design. By using this approach, the optimal structure of a process design as well as all the design and operating parameters for each piece of equipment can all be determined simultaneously. Initially the structure includes multiples redundant paths and equipment alternatives for achieving the design objectives that are set. The mathematical problem is usually modeled as a complex MINLP problem that can be solved using an

optimization program such as GAMS. During the optimization process, it strips away the least useful paths and equipment alternatives. The streams, connections, operating conditions, and other design parameters for each piece of equipment are then determined in one simultaneous mathematical program by optimization of a design criterion. Usually this design criterion is annual cost but other criterions can use as well. If at the optimum solution the flow through some interconnection or the size of a corresponding piece of equipment is zero, then the associated pathway is deleted from the flow sheet. In this fashion both the design structure and other design parameters are then optimized simultaneously. One problem is that optimization can only be achieved if the optimal process pathway was already embedded within the original superstructure.

4.1 Recent Superstructure Research

Recently, Qi and Henson have proposed superstructure schemes with NLP and MINLP technology [Qi and Henson, 2000]. The general-purpose is the first example of a systematic approach for the optimization of gas permeation membrane networks using spiral wound permeators. They used a fixed choice of network pressures and present studies from their experiments with the formulation.

Kokoos extended an earlier superstructure in distillation to account for membrane separation. The mathematical formulation is based on fixed pressures and presents designs in the production of nitrogen and oxygen enriched air and in the separation of CO_2/CH_4 gas mixture [Kookos, 2002]. An example of a superstructure developed by Kookos is shown below.

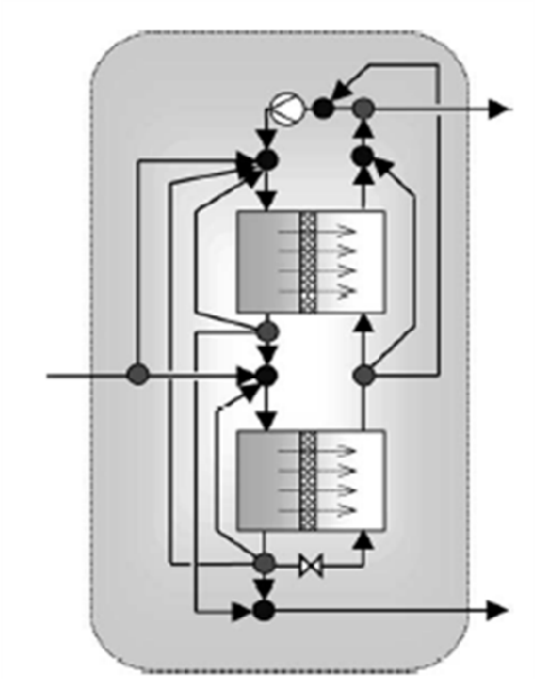

Figure 11: Superstructure Developed by Kookos for Two Stage (Kookos,2002)

4.2 Superstructure Model

Once the model of a single membrane is complete, the next phase is to model the superstructure network of membranes that will be able to accomplish the job of natural gas processing without the use of traditional techniques. Up to this point effective methods of determining efficient combinations of membrane area and numbers of membrane were developed by deciding upon a number of membranes and size, then determining what was the capability of this particular set up, and comparing it to another set up. This method is very time consuming and also prevents a possibility of greater

efficiency if not all possibilities are examined. For example, the following four membrane combinations are possible. The most efficient way to process each membrane combination is to model a superstructure that will optimize the membrane to desired output ratio, instead of analyzing each of these configurations one at a time.

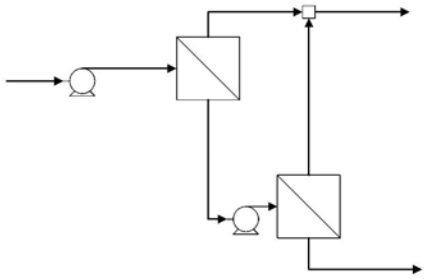

(a) series with permeate re-processing

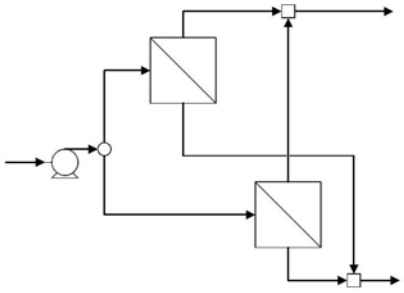

(b) parallel arrangement

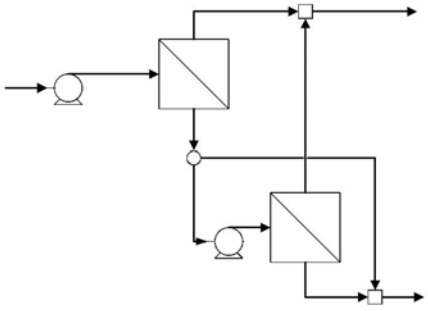

(c) series with permeate bypass, permeate re-processing

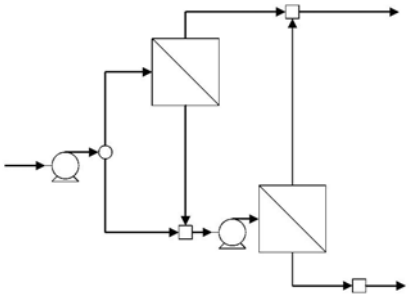

(d) series with feed bypass, permeate re-processing

Figure 13: Various Membrane Design Configuration

An illustration of the proposed superstructure used in our model is shown in **Figure 14**. It encompasses a large number of design configurations for a two-stage membrane network. Each of which is a candidate for the optimal process pathway. The basic components of this superstructure are membranes, compressors, stream mixers and stream splitters. It is similar to the superstructure developed by Henson.

Deleted: permeators

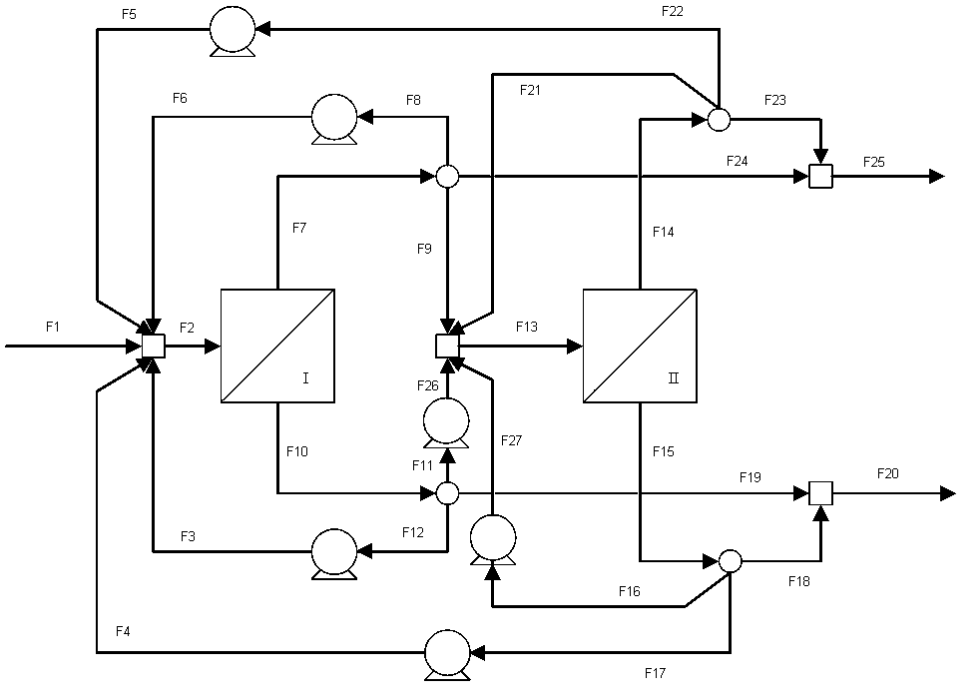

Figure 14: Diagram of Proposed Superstructure

In order for the GAMS model to support various amounts of mixing points and splitting points the following equations were added:

Feed balance(j).. $feed(j)=\Sigma_m fm(j,m);$ **Eq.6**

Feedproportion(j,m).. $= \frac{feed(j)}{\Sigma_l feed(l)} = \frac{fm(j,m)}{\Sigma_l fm(l,m)};$ **Eq.7**

Retentanebalance(j,m).. Σ_k retentateout(k,j,m) = Σ_{ma} frm(j,m,ma) + frout(j,m); **Eq.8**

Retentatecomp(j,m).. Σ_k retentateout(k,j,m) = rc(j,m) * $\Sigma_{k,l}$ retentateout (k,l,m); **Eq.9**

Rmproportion(j,m,ma)..frm(j,m,ma) = rc(j,m) * Σ_l frm(l,m,ma); **Eq.10**

Permeatebalance(m,j)..permeatout(j,m) = Σ_{ma} fpm(j,m,ma)+fpout(j,m); **Eq.11**

Permeatecomp(j,m,ma)..pc(j,m) = xs('l',j,m); **Eq.12**

Pmproportion(j,m,ma)..fpm(j,m,ma) = pc(j,m)* Σ_l fpm(l,m,ma); **Eq.13**

Mixmembrane(j,m).. fin(j,m) = fm(j,m) + Σ_{ma} frm(j,ma,m) + Σ_{ma} fpm(j,ma,m); **Eq.14**

Outretentate(j)..outr(j) = Σ_m frout(j,m); **Eq.15**

Ourproportion(j,m)..frout(j,m) = rc(j,m)* Σ_l frout(l,m); **Eq.16**

Outpermeate(j)..outp(j) = Σ_m fpout (j,m); **Eq.17**

Outproportion..fpout(j,m) = pc(j,m)* Σ_l fpout(l,m); **Eq.18**

Retentatepower(m,ma)..Wrm(m,ma) = Σ_j frm(j,m,ma)*cp*temp* … **Eq.19**

...(((Pt(ma)/Pt(m)**(kf-1/kf))-1);

Permeatepower(m,ma)..Wpm(m,ma) = Σ_j fpm(j,m,ma)*cp*temp*… **Eq.20**

…(((Pt(ma)/Ps(m)**(kf-1/kf))-1);

Membranepower(m)..Wfm(m) = Σ_j fm(j,m)*cp*temp*… **Eq.21**

…((Pt(m)/Pfeed))**(kf-1/kf))-1:

Equations 6-18 are used to describe the mixing and splitting points found in the superstructure. While Equations 19-21 are used to describe the power required to compress the streams of recycled retentate into the feed, the recycled permeate into the feed, and the compression required to compress the mixed feed into the second membrane.

Also included in the GAMS programming was the inclusion of binary variables in order to determine the existence of a given structure or stream. The binary variables are also used to determine the existence of splitting and mixing points.

4.3 Results

In order to obtain an optimum membrane network, we added an objective function to our model to find the most economically efficient membrane network. The objective function we added was **90*Σ area + 180* CO_2 composition in retentate + .0015*Σ power of compressors.** Pressures for both membranes and components were added to the GAMS model. As well as initial components and flow rates. The resulting code from GAMS specifies two membranes with equal areas of 0.44 m^2. The retentate from membrane one is recycled into the first membrane again. The resulting superstructure can be seen in Figure 15. The feasible solution:

```
 ** Feasible solution. Value of objective =    36433.9630660
```

is obtained using MILP (Mixed Integer Linear Programming). The objective equation to minimize was defined as the sum of the cost of the area + the cost of the CO_2 in the retentate + the cost of the compressor. The cost of the area was determined to be $\$90/m^2$. The cost of the loss of methane due to the occupying space of the CO_2 content in the retentate was determined to be \$0.05 per second. The cost of the compressor was determined to be included in the cost of electricity being used to power the compressor. The power is given in kJ/s and with the assumption that electricity is \$0.07 per kilowatt hour. The cost to run the compressors is then determined to be \$540 per hour or \$0.15 per second.

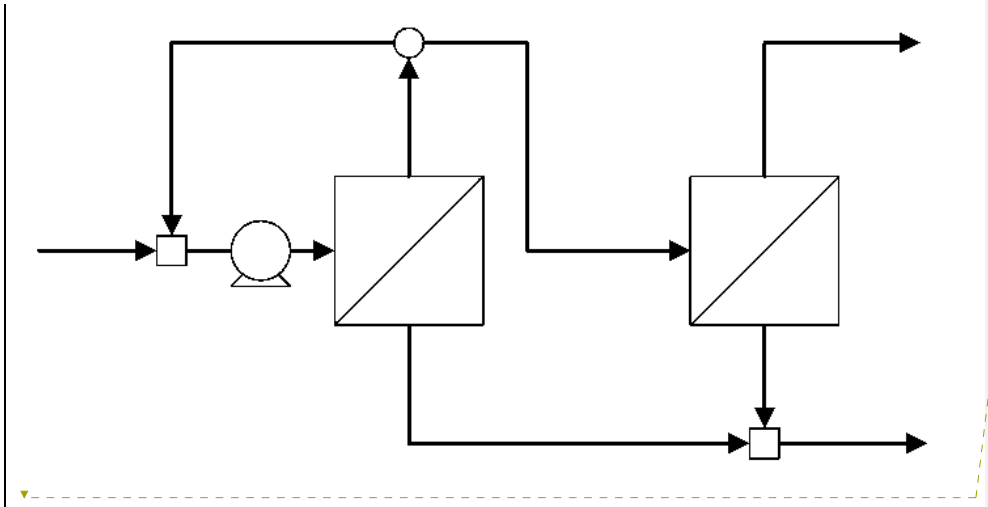

Deleted: ¶
¶

Figure 15: Superstructure Result from GAMS

We added a new objective function and conditions for the process in order to obtain results which would be reasonable and comparable to a standard. In order to do this, we used conditions for the feed and final product and economic factors used in the paper by

Qi and Henson. The conditions for the feed was a total flow rate of 10 mol/s (around .7 MMSCFD) with a composition of 73% methane, 19% carbon dioxide, 1% hydrogen sulfide, and 7% ethane. The condition for the final retentate was a final composition of 2% carbon dioxide or less.

The capital and operating costs were calculated based upon values given by Qi and Henson. The overall objective function contained a capital cost and operating cost portion. The capital cost portion was calculated using the following equations:

$F_{fc} = f_{mh} * \sum Area + f_{cmp} * W_t / \eta$

$F_{tc} = f_{pp} * (1 + f_{wk}) * (F_{fc})$

where η is the efficiency of the compressors (70%), F_{fc} is the fixed capital investment, f_{mh} is the cost of the membrane housing (200\$/m^2), f_{cmp} is the cost of the compressors (1000\$ / kW of required power), f_{wk} is percent of the fixed capital investment needed for working capital (10%), and f_{pp} is the amount of the capital cost that must be paid back each year (27%).

The operating costs were calculated using the following equations:

$F_{mr} = f_{mr} * \sum Area.$

$F_{mt} = f_{mt} * F_{fc}$

$F_{ut} = f_{gp} * W_t / f_{hv} / \eta$

$F_{pl} = f_{gp} * m_p$

Where F_{mr} is the total cost of membrane replacement, f_{mr} is the cost of membrane replacement (\$30/m^2/yr), F_{mt} is the cost of maintenance, f_{mt} is the weighting factor for the maintenance costs (5%), F_{ut} is the total cost of the utilities, f_{gp} is the cost of the natural gas (\$35/Mm^3), f_{hv} is the heating value of the fuel (43MJ/m^3), F_{pl} is the total cost for the

product losses, t_{wk} is the operating days per year (300 days/yr), and m_p is the total flow rate of the product in the permeate.

The total cost is then $F_{total} = F_{tc}+F_{mr}+F_{mt}+t_{wk}*(F_{ut}+F_{pl})$ and is the total annual cost.

The second membrane network that was obtained is shown in Figure 17. Figure 17 is a two membrane network with membranes in parallel. There are similarities to the Qi, and Henson model. (Fig. 16) Namely a fraction of the permeate from the second membrane is recycled to the feed of the first membrane, instead of the entire permeate being sent to the first membrane for further separation. The compressor work values are similar in terms of the amount of natural gas that is compressed. The model results in a work value of 11.35, while Qi and Henson determined compressor work to be 8.31 kWh. A major factor for the discrepancy in values is due to the fact that Qi and Henson used spiral-wound membranes, while the GAMS model was modeled on hollow fiber tubes. This major discrepancy in module membranes also reduced the area in the GAMS model network to 160 m^2 from 380 m^2 in Qi and Henson. The model we found also has higher recovery of methane. The lower area and higher recovery of methane in the hollow fiber model makes the overall cost of the structure we found to be slightly lower than the cost found for Qi and Henson's model. The total cost for our method is \$11.05 per 1000m^3 of gas processed while Qi and Henson's model is about \$11.11 per 1000m^3 of gas processed.

However, the structure found is likely not the true optimum. The model originally would not consider recycles and would obtain fairly high objective functions. Forcing the model to recycle permeate and retentate resulted in much lower objective functions.

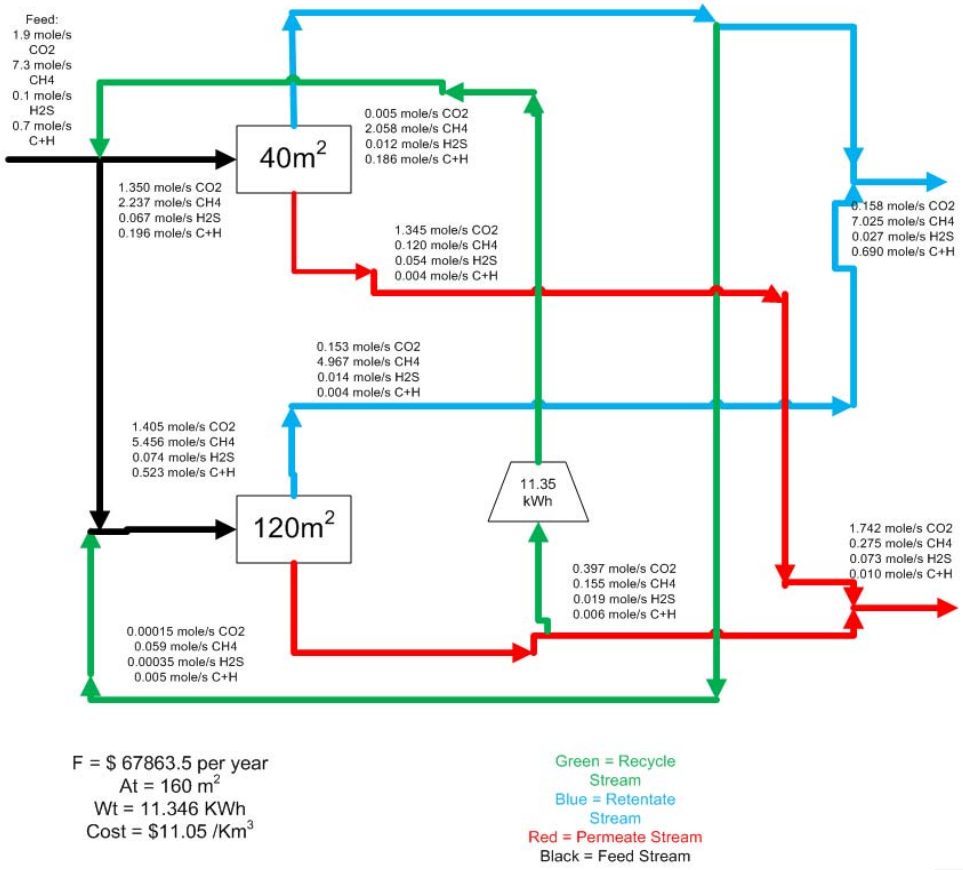

Figure 16: Optimum Network w/Rigorous Objective Function

In order this problem we added a loop function which is shown in figure 18. This loop helped to generate initial guesses for the feed to each membrane as well as the recycles. By running this loop for a large number of cycles, the model would generate many feasible and non-feasible solutions. The lowest of the feasible solutions was selected and used as our optimum model for the membrane network. As such, the validity of our model as the optimum membrane network cannot be asserted.

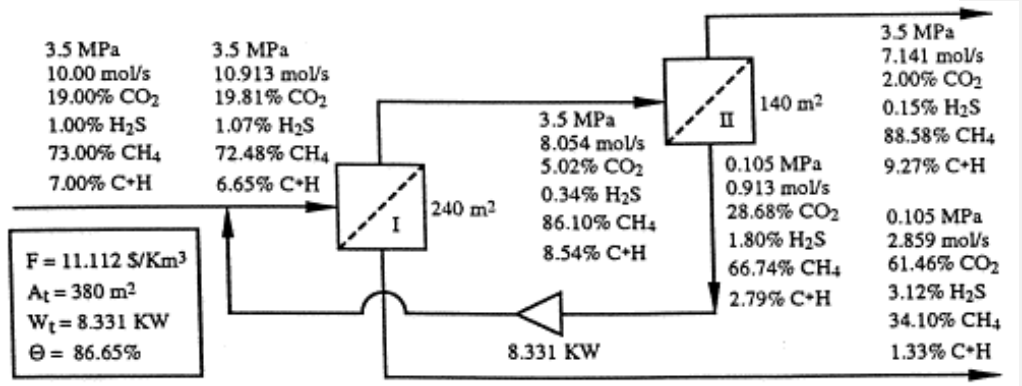

Figure 17: Qi and Henson Optimum Two Membrane Network

```
Parameters cont;
cont=1;
while (cont <= card(c),
*starting points
fm.l('1','1')=uniform(0,Feed('1'));
fm.l(j,'1')$(ord(j)<>1)=feed(j)*Feed('1')/sum(l,feed(l));
fm.l(j,'2')=Feed(j)-fm.l(j,'1');
fpm.l(j,m,ma)=uniform(0,fm.l(j,m));
frm.l(j,m,ma)=uniform(0,fm.l(j,m));
Solve MILP using mip minimize object;
Solve MINLP using minlp minimize object;
Display object.l;
     cont=cont+1;);
```

Figure 18: Initial Guess Generation Loop

Conclusion

The modeling of a two membrane network using a MINLP model was successful. The final retentate met the specification of 2% CO_2 or less in the final retentate and the results showed some similarity with previous work on membrane network optimization. Some discrepancy between the two sets of results can be expected since the types of membranes

modeled were different; however, considering the model could not generate the optimum without the use of initial guesses, the model is likely only a local minimum rather a global minimum in the cost function.

Future work would include additional refining of the model to make it more rigorous, consideration of membrane networks which consider a larger number of membranes, and possibly the consideration of new, highly efficient “thermally rearranged” membranes when technical information (particularly cost) is published.

References

Qi., R., Henson, M.A., 'Optimization-based design of spiral-wound membranes systems for CO2/CH4 separations', Separation and Purification Technology, 13, 209-225, 1998

Qi., R., Henson, M.A., 'Membrane system design for multicomponent gas mixtures via mixed-integer nonlinear programming',Computers and Chemical Engineering, 24, 2719-2737, 2000

Qi, R. and M. A. Henson, "Approximate Modeling of Spiral-Wound Gas Permeators," Journal of Membrane Science, 121, 11-24, 1996

Qi, R. and M. A. Henson, "Modeling of Spiral-Wound Permeators for Multicomponent Gas Separations," Industrial Engineering and Chemistry Research, 36, 2320-2331, 1997

Kookos, I.K., 'A targeting approach to the synthesis of membrane network for gas separations', j. Membrane Science, 208, 193-202, 2002

Baker, R.W., 'Future directions of membrane gas separation technology', *Ind. Eng. Chem. Res*., 2002, 41, 1393-1411

Mark C. Porter, "Handbook of Industrial Membrane Technology", Westwood, New Jersey, Noyes Publications, 1990.

Seader, J. D., and Henley, E. J. "Separation Process Principles". New York: John Wiley & Sons, Inc., 1998.

'Basic Principles of Membrane Technology', Mulder, M., 2nd. Edt., Kluwer Academic Publishers, 1996

Natural Gas Supply Association, http://www.naturalgas.org/index.asp

John A. Howell, The Watt Committee on Energy, "The Membrane Alternative", London Polymeric Gas Separation Membranes by Donald R. Paul, Yuri P. Yampolskii, 1996.

Baker, R.W., 'Future directions of membrane gas separation technology', *Ind. Eng. Chem. Res*., 2002, 41, 1393-1411

http://energy.cr.usgs.gov/energy/stats_ctry/Stat1.html#CONSUMPTION

Dortmund, D., Doshi, K., 'Recent Developments in CO_2 Removal Membrane Technology, http://www.uop.com/gasprocessing/TechPapers/CO2RemovalMembrane.pdf

Aquilo Gas Separation bv; http://www.aquilo.nl/products.htm

Filtration Solutions Inc., http://www.filtsol.com/technology/super_hydrophilic.shtml

Appendix

```
SET
    m set of components /1,2/
    j set of components /1,2,3,4/
    k set of segments /1*30/
    d set of discretized concentrations /1*3/
    c set of counting /1*20/;
*j=1 is CO2 and j=2 is CH4 , j=3 is H2S, and j=4 is C+H
alias(j,l),(k,ka),(m,ma);


SCALAR
*Vtot     Total volumetric flowrate (cm^3 per sec) /0.002619/
*Pt       Tube side Pressure (MPa) /100/
*Ps       Shell side Pressure (MPa) /.105/
dm        Thickness of membrane (m)/1/
dout      Outer diameter of shell (m)/.0003/
din       Inner diameter of inside (m)/0.000150/
pi        This is pi /3.14/
dlm       Log mean diameter (m) /0.0003952/
*oflux     optimum flux /.0089/
dT        Amount of tubes /6130/
Zin       Availible Length (m) /100/
dz        Delta z (m)          / 1 /
Pfeed     Pressure feed (Mpa)    /3.5/
R         Heat capacity Kj per mole times sec /.0083144/
Temp      Temperature kelvin /313/
kf        compressibility factor /1.3/
rcomp     %CO2 in final retentate /.02/
;
PARAMETER
Pt(m)  Tube side Pressure (MPa)
       /1   3.5
        2   3.5/

Ps(m)  Shell side Pressure (MPa)
        /1    .105
         2    .105/

Feed(j)  Feed flowrate of each component
      /1  1.9
       2  7.3
       3  .1
       4  .7/
** (mol/s)
dxt(d),dxs(d),da,Z,CC;
```

```
Table Q(m,j)  permeability divided by thickness
     1           2           3           4
1    2.96E-2     1.48E-3     2.368E-2    5.92E-4
2    2.96E-2     1.48E-3     2.368E-2    5.92E-4;
*3    2.96E-2     1.48E-3     2.368E-2    5.92E-4;
*barrer
```

```
VARIABLES
dJ(k,j,m)          Rate of transport
xs(k,j,m)          Mole fraction of j shell side at k
xt(k,j,m)          Mole fraction of j tube side at k
ft(k,j,m)          Component Material balance tube side
fs(k,j,m)          Component Material balance shell side
fm(j,m)            Flow from feed to membrane
frout(j,m)
fpout(j,m)
outr(j)
outp(j)
sigT(k,m)          Total flow rate tube side
sigS(k,m)          Total flow rate shell side
ftin(j,m)          Inlet flowrate of component j in membrane m
retenteout(k,j,m)
permeateout(j,m)
frm(j,m,m)
fpm(j,m,m)
rc(j,m)
pc(j,m)
object             Objective value
Area(m)            Total Area
Wrm(m,ma)
Wpm(m,ma)
Wfm(m)
;
```

```
POSITIVE VARIABLES dJ,rc,pc,xt,xs,fm,ft,fs,sigT,sigS,Area,retenteout,
permeateout,frm,fpm,rc,pc,frout,fpout,outr,outp,Wrm,Wpm,Wfm;
Binary variables yt(k,j,d,m),ys(k,j,d,m),yk(k,m),yrc(j,m,d),ypc(j,m,d);
xs.up(k,j,m)=1;
xt.up(k,j,m)=1;

*Bounds
dJ.up(k,j,m)=feed(j);
fm.up(j,m)=feed(j);
ft.up(k,j,m)=feed(j);
fs.up(k,j,m)=feed(j);
frout.up(j,m)=feed(j);
fpout.up(j,m)=feed(j);
outr.up(j)=feed(j);
outp.up(j)=feed(j);
sigT.up(k,m)=10;
sigS.up(k,m)=10;
retenteout.up(k,j,m)=feed(j);
permeateout.up(j,m)=feed(j);
frm.up(j,m,m)=feed(j);
fpm.up(j,m,m)=feed(j);
rc.up(j,m)=1;
pc.up(j,m)=1;

yt.fx(k,j,d,m)$(ord(d)=card(d))=0;
ys.fx(k,j,d,m)$(ord(d)=card(d))=0;

*Calculation of the discretized parameter
dxt(d)=(ord(d)-1)*(1/(card(d)-1));
dxs(d)=(ord(d)-1)*(1/(card(d)-1));
Z=Zin;
*dA=dT*pi*dlm*Z/(card(k)-1);
dA=20 ;
display dA;


*retenteout.fx('1')=8;
*yk.fx('10')=1;
*Area.up=500;

*ftin.fx(j,m)=feed(j);
*fpm.lo(j,'2','1')=0.2;
```

```
EQUATIONS
Rate_of_Transport1  Rate of transport
Rate_of_Transport2  Rate of transport
Rate_of_Transport3  Rate of transport
Rate_of_Transportk1 Rate of transport
Rate_of_Transportk2 Rate of transport
CMBTube_1           Component Material Balance (tube side)
CMBTube1            Component Material Balance (tube side)
CMBTube2            Component Material Balance (tube side)
ret                 Retentate equation
CMBShell_1          Component Material Balance (shell side)
CMBShell_2          Component Material Balance (shell side)
CMBShell1           Component Material Balance (shell side)
CMBShell2           Component Material Balance (shell side)
perm                Permeate equation
MFJShell            Mole fraction of j shell side
MFJTube             Mole fraction of j tube side
TFTube              Total flow tube side of second component
TFShell             Total flow shell side of second component
TotalArea           Total Area calculation
objectivefunction   Objective variable
daequation
dimension
zerofs
zeroft
Retentatepower
Permeatepower
Membranepower

******Mixer and splitter balances
feedbalance
feedproportion
retentatebalance
retentatecomp
rmproportion
permeatebalance
permeatecomp
pmproportion
mixmembrane
outretentate
outrproportion
outpermeate
```

```
****Discrete equations
lowerboundMFJTube
upperboundMFJTube
discreteMFJTube
upperxt
lowerxt
lowerboundMFJShell
upperboundMFJShell
discreteMFJShell
upperxs
lowerxs
lowerretentatecomp
upperretentatecomp
lowerrmproportion
upperrmproportion
lowerpmproportion
upperpmproportion
loweroutrproportion
upperoutrproportion
loweroutpproportion
upperoutpproportion
sumyrc
sumypc
CO2comp
CO2comp2 ;

* Use the GAMS ORD (ordinality) and CARD (cardinality)
*functions to automate the identification of the first
*and last periods of the model horizon:

Rate_of_Transport1(k,j,m)   .. dJ(k,j,m)-Q(m,j)*((xt(k,j,m)*Pt(m))-(xs(k+1,j,m)*Ps(m)))=G=-1*sum(ka$(ord(ka)<=ord(k)),yk(ka,m));
Rate_of_Transport2(k,j,m)   .. dJ(k,j,m)-Q(m,j)*((xt(k,j,m)*Pt(m))-(xs(k+1,j,m)*Ps(m)))=L=10*sum(ka$(ord(ka)<=ord(k)),yk(ka,m));
Rate_of_Transport3(k,j,m)   .. dJ(k,j,m)=L=10*sum(ka$(ord(ka)>=ord(k)),yk(ka,m));
Rate_of_Transportk1(k,j,m)  .. dJ(k,j,m)-Q(m,j)*((xt(k,j,m)*Pt(m))-(xs(k,j,m)*Ps(m)))=G=-1*(1-yk(k,m));
Rate_of_Transportk2(k,j,m)  .. dJ(k,j,m)-Q(m,j)*((xt(k,j,m)*Pt(m))-(xs(k,j,m)*Ps(m)))=L=10*(1-yk(k,m));

CMBShell_1(k,j,m)           ..fs(k,j,m)-dJ(k,j,m)*dA=G=-1*(1-yk(k,m));
CMBShell_2(k,j,m)           ..fs(k,j,m)-dJ(k,j,m)*dA=L=10*(1-yk(k,m));
CMBShell1(k,j,m)            ..fs(k,j,m)-fs(k+1,j,m)-dJ(k,j,m)*dA=G=-1*sum(ka$(ord(ka)<=ord(k)),yk(ka,m));
CMBShell2(k,j,m)            ..fs(k,j,m)-fs(k+1,j,m)-dJ(k,j,m)*dA=L=100*sum(ka$(ord(ka)<=ord(k)),yk(ka,m));
perm(j,m)                   ..permeateout(j,m)=e=fs('1',j,m);
zerofs(k,j,m)               ..fs(k,j,m)=L=feed(j)*sum(ka$(ord(ka)>=ord(k)),yk(ka,m));
```

```
MFJTube(k,j,m)              ..xt(k,j,m)*(sigT(k,m))=E= ft(k,j,m);
MFJShell(k,j,m)             ..xs(k,j,m)*(sigS(k,m))=E= fs(k,j,m);

TFTube(k,m)                 ..sigT(k,m)=e=sum(j,ft(k,j,m));
TFShell(k,m)                ..sigS(k,m)=e=sum(j,fs(k,j,m));
TotalArea(m)                ..Area(m)=E=sum(k,yk(k,m)*(ord(k)-1))*dA;

*objectivefunction           ..object=e=-sum(m,fs('1','1',m));
objectivefunction           ..object=e=.27*1.10*((200*sum(m,Area(m)))+sum((m,ma),Wpm(m,ma))*1000+sum(m,Wfm(m))*1000)
+30*sum(m,Area(m))+300/365*((200000*outp('2'))+38.8*sum(m,Wfm(m))+(sum((m,ma),Wrm(m,ma)+Wpm(m,ma)))*38.8);
dimension(m)                ..sum(k,yk(k,m))=E=1;

******Mixer and splitter balances
feedbalance(j)              ..feed(j)=E=sum(m,fm(j,m));
feedproportion(j,m)         ..feed(j)*sum(l,fm(l,m))=E=sum(l,feed(l))*fm(j,m);
retentatebalance(j,m)       ..sum(k,retenteout(k,j,m))=E=sum(ma,frm(j,m,ma))+frout(j,m);
retentatecomp(j,m)          ..sum(k,retenteout(k,j,m))=E=rc(j,m)*sum((k,l),retenteout(k,l,m));
rmproportion(j,m,ma)        ..frm(j,m,ma)=E=rc(j,m)*sum(l,frm(l,m,ma));
permeatebalance(m,j)        ..permeateout(j,m)=E=sum(ma,fpm(j,m,ma))+fpout(j,m);
permeatecomp(j,m,ma)        ..pc(j,m)=E=xs('1',j,m);
CO2comp(j,m)                ..outr('1')=l=rcomp*sum(l,outr(l));
*CO2comp2(j,m)               ..outr('1')=l=rcompup*sum(l,outr(l));
pmproportion(j,m,ma)        ..fpm(j,m,ma)=E=pc(j,m)*sum(l,fpm(l,m,ma));
mixmembrane(j,m)            ..ftin(j,m)=E=fm(j,m)+sum(ma,frm(j,ma,m))+sum(ma,fpm(j,ma,m));
outretentate(j)             ..outr(j)=e=sum(m,frout(j,m));
outrproportion(j,m)         ..frout(j,m)=E=rc(j,m)*sum(l,frout(l,m));
outpermeate(j)              ..outp(j)=E=sum(m,fpout(j,m));
outpproportion(j,m)         ..fpout(j,m)=E=pc(j,m)*sum(l,fpout(l,m));

****Compressors Power
Retentatepower(m,ma)        ..Wrm(m,ma)=e=sum(j,frm(j,m,ma))*R*Temp*(log(Pt(ma)/Pt(m)));
Permeatepower(m,ma)         ..Wpm(m,ma)=e=sum(j,fpm(j,m,ma))*R*Temp*(log(Pt(ma)/Ps(m)));
Membranepower(m)            ..Wfm(m)=e=sum(j,fm(j,m))*R*Temp*(log(Pt(m)/Pfeed));
```

```
****Discrete equations
lowerboundMFJTube(k,j,d,m)  ..ft(k,j,m)=G=(sigT(k,m))*dxt(d)-100*(1-yt(k,j,d,m)) ;
upperboundMFJTube(k,j,d,m)  ..ft(k,j,m)=L=(sigT(k,m))*dxt(d+1)+feed(j)*(1-yt(k,j,d,m)) ;
discreteMFJTube(k,j,m)      ..sum(d,yt(k,j,d,m))=E=sum(ka$(ord(ka)>ord(k)),yk(ka,m));
upperxt(k,j,m)              ..xt(k,j,m)=L=sum(d,dxt(d+1)*yt(k,j,d,m));
lowerxt(k,j,m)              ..xt(k,j,m)=G=sum(d,dxt(d)*yt(k,j,d,m));
lowerboundMFJShell(k,j,d,m)..fs(k,j,m)=G=(sigS(k,m))*dxs(d)-100*(1-ys(k,j,d,m)) ;
upperboundMFJShell(k,j,d,m)..fs(k,j,m)=L=(sigS(k,m))*dxs(d+1)+feed(j)*(1-ys(k,j,d,m)) ;
discreteMFJShell(k,j,m)     ..sum(d,ys(k,j,d,m))=E=sum(ka$(ord(ka)>ord(k)),yk(ka,m));
upperxs(k,j,m)              ..xs(k,j,m)=L=sum(d,dxs(d+1)*ys(k,j,d,m));
lowerxs(k,j,m)              ..xs(k,j,m)=G=sum(d,dxs(d)*ys(k,j,d,m));
lowerretentatecomp(j,m,d)   ..sum(k,retenteout(k,j,m))=G=sum((k,l),retenteout(k,l,m))*dxt(d)-100*(1-yrc(j,m,d));
upperretentatecomp(j,m,d)   ..sum(k,retenteout(k,j,m))=L=sum((k,l),retenteout(k,l,m))*dxt(d)+feed(j)*(1-yrc(j,m,d));
lowerrmproportion(j,m,ma,d)..frm(j,m,ma)=G=sum(l,frm(l,m,ma))*dxt(d)-100*(1-yrc(j,m,d));
upperrmproportion(j,m,ma,d)..frm(j,m,ma)=L=sum(l,frm(l,m,ma))*dxt(d)+feed(j)*(1-yrc(j,m,d));
lowerpmproportion(j,m,ma,d)..fpm(j,m,ma)=G=sum(l,fpm(l,m,ma))*dxt(d)-100*(1-ypc(j,m,d)); ;
upperpmproportion(j,m,ma,d)..fpm(j,m,ma)=L=sum(l,fpm(l,m,ma))*dxt(d)+feed(j)*(1-ypc(j,m,d));
loweroutrproportion(j,m,d)  ..frout(j,m)=G=sum(l,frout(l,m))*dxt(d)-100*(1-yrc(j,m,d));
upperoutrproportion(j,m,d)  ..frout(j,m)=L=sum(l,frout(l,m))*dxt(d)+feed(j)*(1-yrc(j,m,d));
loweroutpproportion(j,m,d)  ..fpout(j,m)=G=sum(l,fpout(l,m))*dxt(d)-100*(1-yrc(j,m,d));
upperoutpproportion(j,m,d)  ..fpout(j,m)=L=sum(l,fpout(l,m))*dxt(d)+feed(j)*(1-yrc(j,m,d));
sumyrc(j,m)                 ..sum(d,yrc(j,m,d))=L=1;
sumypc(j,m)                 ..sum(d,ypc(j,m,d))=L=1;
```

```
Model GreaterArea /all/;
Model MILP /Rate_of_Transport1,Rate_of_Transport2,Rate_of_Transport3,Rate_of_Transportk1,Rate_of_Transportk2,
CMBTube_1,CMBTube1,CMBTube2,ret,CMBShell1,CMBShell2,perm,TFTube,TFShell,TotalArea,objectivefunction,CMBShell_1,CMBShell_2,
lowerboundMFJTube,upperboundMFJTube,discreteMFJTube,lowerboundMFJShell,upperboundMFJShell,discreteMFJShell,upperxt,
lowerxt,upperxs,lowerxs,dimension,zerofs,zeroft,
feedbalance,feedproportion,retentatebalance,permeatebalance,permeatecomp,mixmembrane,outretentate,outpermeate,
lowerretentatecomp,lowerrmproportion,lowerpmproportion,loweroutrproportion,loweroutpproportion,
upperretentatecomp,upperrmproportion,upperpmproportion,upperoutrproportion,upperoutpproportion,sumyrc,sumypc,
Retentatepower,Permeatepower,Membranepower,CO2comp/;
*CMBShell_1
```

```
Model RMINLP /Rate_of_Transport1,Rate_of_Transport2,Rate_of_Transport3,Rate_of_Transportk1,Rate_of_Transportk2,
CMBTube_1,CMBTube1,CMBTube2,ret,CMBShell1,CMBShell2,perm,MFJShell,MFJTube,CMBShell_1,CMBShell_2,
TFTube,TFShell,TotalArea,objectivefunction,dimension,zerofs,zeroft,
feedbalance,feedproportion,retentatebalance,retentatecomp,rmproportion,permeatebalance,permeatecomp,pmproportion,
mixmembrane,outretentate,outrproportion,outpermeate,outpproportion,
Retentatepower,Permeatepower,Membranepower,CO2comp/;
Model MINLP /Rate_of_Transport1,Rate_of_Transport2,Rate_of_Transport3,Rate_of_Transportk1,Rate_of_Transportk2,
CMBTube_1,CMBTube1,CMBTube2,ret,CMBShell1,CMBShell2,perm,MFJShell,MFJTube,CMBShell_1,CMBShell_2,
TFTube,TFShell,TotalArea,objectivefunction,dimension,zerofs,zeroft,
feedbalance,feedproportion,retentatebalance,retentatecomp,rmproportion,permeatebalance,permeatecomp,pmproportion,
mixmembrane,outretentate,outrproportion,outpermeate,outpproportion,
Retentatepower,Permeatepower,Membranepower,CO2comp/;

option iterlim=1000000;
*MILP.optfile=1;
MINLP.optfile=1;
*starting points
fm.l('1','1')=uniform(0,Feed('1'));
fm.l(j,'1')$(ord(j)<>1)=feed(j)*Feed('1')/sum(1,feed(1));
fm.l(j,'2')=Feed(j)-fm.l(j,'1');
frm.l(j,m,ma)=uniform(0,fm.l(j,m));

Solve MILP using mip minimize object;
*object.lo=object.l;
*Solve RMINLP using rminlp minimize object;
Solve MINLP using minlp minimize object;

Parameters cont;
cont=1;
while (cont <= card(c),
*starting points
fm.l('1','1')=uniform(0,Feed('1'));
fm.l(j,'1')$(ord(j)<>1)=feed(j)*Feed('1')/sum(1,feed(1));
fm.l(j,'2')=Feed(j)-fm.l(j,'1');
fpm.l(j,m,ma)=uniform(0,fm.l(j,m));
frm.l(j,m,ma)=uniform(0,fm.l(j,m));
Solve MILP using mip minimize object;
Solve MINLP using minlp minimize object;
Display object.l;
     cont=cont+1;);
```